Since January 2020 Elsevier has created a COVID-19 resource centre with free information in English and Mandarin on the novel coronavirus COVID-19. The COVID-19 resource centre is hosted on Elsevier Connect, the company's public news and information website.

Virology 464-465 (2014) 432–440

Contents lists available at ScienceDirect

Virology

journal homepage: www.elsevier.com/locate/yviro

The interaction of nonstructural protein 9 with retinoblastoma protein benefits the replication of genotype 2 porcine reproductive and respiratory syndrome virus *in vitro*

Jianguo Dong, Ning Zhang, Xinna Ge, Lei Zhou, Xin Guo*, Hanchun Yang*

Key Laboratory of Animal Epidemiology and Zoonosis of the Ministry of Agriculture, College of Veterinary Medicine and State Key Laboratory of Agrobiotechnology, China Agricultural University, Beijing, People's Republic of China

ARTICLE INFO

Article history:
Received 23 April 2014
Returned to author for revisions
18 July 2014
Accepted 21 July 2014
Available online 21 August 2014

Keywords:
Porcine reproductive and respiratory syndrome virus (PRRSV)
Genotype 2
Nonstructural protein 9 (Nsp9)
Retinoblastoma protein (pRb)
Interaction
Replication

ABSTRACT

The nonstructural protein 9 (Nsp9) of porcine reproductive and respiratory syndrome virus (PRRSV) is a RNA-dependent RNA polymerase (RdRp) that plays a vital role in viral replication. This study first demonstrated that the Nsp9 of genotype 2 PRRSV interacted with cellular retinoblastoma protein (pRb), and Nsp9 co-localized with pRb in the cytoplasm of PRRSV-infected MARC-145 cells and pulmonary alveolar macrophages (PAMs). Next, the overexpression of truncated pRb was shown to inhibit the PRRSV replication and silencing the pRb gene could facilitate the PRRSV replication in MARC-145 cells. Finally, the pRb level was confirmed to be down-regulated in PRRSV-infected MARC-145 cells, and Nsp9 was shown to promote the pRb degradation by proteasome pathway. These findings indicate that the interaction of Nsp 9 with pRb benefits the replication of genotype 2 PRRSV *in vitro*, helping to understand the roles of Nsp9 in the replication and pathogenesis of PRRSV.

Introduction

Porcine reproductive and respiratory syndrome (PRRS) is an important viral disease that brings about great economic losses to the pig industry worldwide (Garner et al., 2001; Neumann et al., 2005; Pejsak et al., 1997). The causative agent, PRRS virus (PRRSV), belongs to the *Arterivirus* genus of the *Arteriviridae* family, together with equine arteritis virus (EAV), lactate dehydrogenase-elevating virus (LDV) and simian hemorrhagic fever virus (SHFV) (Cavanagh, 1997). The PRRSV is divided into two major genotypes, genotype 1 (European) and genotype 2 (North American) (Nelson et al., 1993). Clinically, the viruses of the two genotypes cause a similar syndrome although they share only approximately 60% nucleotide identity of the genome (Meng et al., 1995; Nelson et al., 1993). In China, a highly pathogenic PRRSV (HP-PRRSV) of genotype 2 was recognized to cause atypical PRRS outbreaks in the pig-producing areas in 2006 (Tian et al., 2007; Zhou and Yang, 2010). A recent investigation indicated that the HP-PRRSV has become the dominating virus circulating in pig farms during the past years (Zhou et al., 2014).

The PRRSV genome is a single strand positive RNA with approximately 15 kb in length, which encodes at least ten open reading frames (ORFs) comprising of ORF1a, ORF1b, ORF2a, ORF2b, ORFs3–7 and the newly discovered ORF5a (Conzelmann et al., 1993; Firth et al., 2011; Johnson et al., 2011; Snijder and Meulenberg, 1998). ORF1a and ORF1b, the replicase-associated genes, encode two polyproteins pp1a and pp1ab, respectively. The pp1a is predicated to be cleaved into ten non-structural proteins (Nsps) including Nsp1α, Nsp1β, Nsp2 to Nsp6, Nsp7α, Nsp7β and Nsp8 (den Boon et al., 1995; Fang and Snijder, 2010; Snijder and Meulenberg, 1998; van Aken et al., 2006), whereas the pp1ab can be cleaved into four Nsps, Nsp9, Nsp10, Nsp11 and Nsp12, which are considered to be involved in viral replication and genomic transcription (Snijder and Meulenberg, 1998; van Dinten et al., 1996; Wassenaar et al., 1997). The transframe fusion (TF) in Nsp2-coding region was recently discovered (Fang et al., 2012). In recent years, a growing number of studies have paid much attention to the pathogenesis involved by the Nsps of PRRSV. The Nsp1, Nsp2, Nsp4 and Nsp11 of PRRSV have been shown to inhibit the induction of type I interferon and modulate host innate immune response (Beura et al., 2010; Han et al., 2013; Kim et al., 2010; Sun et al., 2010, 2012). Moreover, the Nsp1β of PRRSV was shown to interact with the cellular poly(C)-binding protein (PCBP) 1 and 2, and this interaction could facilitate viral replication and RNA transcription (Beura et al., 2011; Wang et al., 2012). A latest study indicated that the PRRSV Nsp4 could induce apoptosis dependent on its 3C-like serine protease activity (Tripp et al., 2013).

* Corresponding authors: College of Veterinary Medicine, China Agricultural University, No. 2 Yuanmingyuan West Road, Haidian District, Beijing 100193, People's Republic of China. Tel./fax: +86 10 6273 1296.
E-mail addresses: guoxin@cau.edu.cn (X. Guo), yanghanchun1@cau.edu.cn (H. Yang).

http://dx.doi.org/10.1016/j.virol.2014.07.036
0042-6822/

The Nsp9 of PRRSV, a RNA-dependent RNA polymerase (RdRp), is considered to be a major component of membrane-associated viral replication and transcription complex (RTC) that is important for virus replication based on the studies of the equine arteritis virus (EAV) and comparative sequence analysis (Pedersen et al., 1999). The SDD motif of Nsp9 has been recognized to be critical for its polymerase activity and virus transcription (Zhou et al., 2011). In addition to its polymerase activity, the interaction between Nsp9 and the host cellular proteins that affect viral replication is poorly understood although a recent study revealed that Nsp9 could interact with endogenous annexin A2 in PRRSV-infected MARC-145 cells (J. Li et al., 2014). Moreover, our recent publication has shown that Nsp9 and Nsp10 together not only affected the HP-PRRSV replication and growth *in vitro and in vivo*, but also contributed to its fatal virulence for piglets (Y. Li et al., 2014). Thus, further exploring the interaction of Nsp9 with host cellular protein (s) is essential for understanding the roles of Nsp9 in the replication and pathogenesis of HP-PRRSV.

The retinoblastoma protein (pRb) encoded by the retinoblastoma tumor suppressor gene has been shown to modulate cell cycle and suppress human tumors (Khidr and Chen, 2006; Weinberg, 1995). The proteins that bind to pRb have been recognized to share a conserved motif—LxCxE (Dahiya et al., 2000), which was first identified in the oncoproteins of DNA tumor viruses (Boyer et al., 1996; White and Khalili, 2006; Whyte et al., 1988). Some proteins of RNA viruses have been shown to bind to pRb through this motif. The interaction between the Rubella virus Nsp9 and pRb could affect viral replication (Forng and Atreya, 1999). In coronavirus, the endoribonuclease Nsp15 could bind to pRb, resulting in the acceleration of cell cycle progression (Bhardwaj et al., 2012). Interestingly, the NS5B of hepatitis C virus (HCV), an RdRp, could interact with pRb and down-regulated the pRb level (Munakata et al., 2005, 2007). In the present study, we explored the interaction between the Nsp9 of genotype 2 PRRSV and pRb and analyzed the effect of this interaction on viral replication *in vitro*.

Results

The Nsp9 of genotype 2 PRRSV interacted with pRb

The conserved LxCxE motif is a key feature for viral proteins that bind to pRb (Dahiya et al., 2000). We aligned the amino acid sequences of the Nsp9 among 17 representative strains of genotype 2 PRRSV and found that the Nsp9 of all the analyzed viruses shared an identical LxCxE motif—LACAE (Table 2). To analyze whether the Nsp9 of genotype 2 PRRSV interacts with pRb through the LACAE motif, the recombinant lentiviruses that were expressing Nsp9-GFP, Nsp9 (L415A/C417A)–GFP and Nsp9 (E419K)–GFP were constructed. MARC-145 cells were transduced with the lentiviruses and the cell lysates were immunoprecipitated with an anti-GFP mAb, and were then detected with an anti-pRb mAb by Co-IP assay. The GFP-expressing lentiviruses were used as the control. As shown in Fig. 1A, the endogenous pRb could be probed in the cells that were expressing Nsp9-GFP and Nsp9 (L415A/C417A)–GFP, whereas it could not be examined in the cells that were expressing Nsp9 (E419K)–GFP, indicating that Nsp9 interacts with pRb and the third conserved residue (E) of the LACAE motif plays a crucial role in sustaining the interaction between Nsp9 and pRb. To further confirm the interaction of Nsp9 with the exogenous pRb, HEK 293T cells were co-transfected with the Myc-pRb-tru-expressing plasmid together with the HA-Nsp9-, HA-Nsp9 (L415A/C417A)- or HA-Nsp9 (E419K)-expressing plasmids, and Co-IP assays were performed. The similar results were obtained (Fig. 1B). Our results suggest that the LACAE motif indeed plays a critical role in the interaction between the viral Nsp9 and pRb.

The Nsp9 of genotype 2 PRRSV co-localized with pRb in the cytoplasm

To analyze the co-localization of Nsp9 and pRb, MARC-145 cells were co-transfected with pCMV-HA-Nsp9 and pCMV-Myc-pRb-tru. The confocal immunofluorescence assays showed that Nsp9 primarily co-localized with pRb-tru in the cytoplasm (Fig. 2A), and the endogenous pRb also co-localized with Nsp9 in the cytoplasm of PRRSV-infected MARC-145 cells (Fig. 2B) and PAMs (Fig. 2C); whereas the endogenous pRb localized in the nucleus of mock-infected MARC-145 cells and PAMs (Figs. 2D and E).

The pRb could inhibit the replication of genotype 2 PRRSV in vitro

To investigate the effect of pRb on the replication of PRRSV, we first analyzed the effect of the exogenous pRb overexpression on the replication of PRRSV. MARC-145 cells were transduced with the pRb-tru-expressing lentiviruses, and were then infected with the PRRSV JXwn06. The virus titers were assayed. As shown in Fig. 3A, the virus titers in the pRb-tru-overexpressing group significantly reduced at the different time points compared with the control group ($p < 0.001$), indicating that the overexpression of pRb-tru can inhibit the replication of PRRSV *in vitro*. To further confirm this effect, MARC-145 cells were individually transfected with three different siRNAs specific for the pRb gene. Western blotting analysis showed that the pRb level in MARC-145 cells was effectively down-regulated by these siRNA compared with the cells transfected with the control (siCon) siRNA (Figs. 3B and C). One pair of siRNA (sipRb2) was used for subsequent experiment.

Table 1
Primers used in this study.

Primer[a]	Sequence(5′-3′)[b]	Product length (bp)	Use
1F	AGCTTTGTTTAAACACCATGTCTCTTGGAATTGT(*Pme*I)	1914	pRb-tru fragment amplification and clone
1R	CGCGCGACGCGTAACTTTTCTTCCCTGTTCG(*Mlu*I)		
2F	CCGGAATTCGGTCTCTTGGAAATTGTAGCCTC(*Eco*RI)	1914	pRb-tru fragment amplification and clone
2R	CGGGGTACCTCACTTTTCTTCCCTGTTCG(*Kpn*I)		
3F	AGCTTTGTTTAAACACCATGCTAGCCGCCAGCGGCTTGAC(*Pme*I)	1920	Nsp9 amplification and clone
3R	CGCGCGACGCGTAACTCATGATTGGACCTGAGTT(*Mlu*I)		
4F	GGAGGAAGATCTCTCTAGCCGCCAGCGGCTTGAC(*Bgl*II)	1920	Nsp9 amplification and clone
4R	TAGTTTAGCGGCCGCTCACTCATGATTGGACCTGAG(*Not*I)		
5F	AATCTTCTTTATGAAGCCGCCGCTGCTGAGGAGCATCTAC		Mutagenesis of Nsp9 (L415A/C417A)
5R	GTAGATGCTCCTCAGCA*GC*GGCG*GC*TTCATAAAGAAGATT		
6F	TGAACTCGAATGTGCT*A*AGGAGCATCTACCGTCGTAC		Mutagenesis of Nsp9 (E419K)
6R	GTACGACGGTAGATGCTCCT*T*AGCACATTCGAGTTCA		

[a] *F* denotes forward PCR primer; *R* denotes reverse PCR primer.
[b] Restriction sites are underlined. Mutated nucleotides are shown as italics.

The MARC-145 cells silenced with sipRb2 were infected with the virus and the virus titers were measured. The results showed that the virus titers of the sipRb2-silenced group were significantly higher than those of the control (siCon) group ($p < 0.001$ or $p < 0.01$) (Fig. 3D), indicating that silencing the pRb gene in MARC-145 cells facilitate the viral replication. The above findings suggest that pRb can inhibit the replication of genotype 2 PRRSV.

Genotype 2 PRRSV infection down-regulated the pRb level

The change of the pRb abundance in MARC-145 cells was analyzed following the PRRSV infection. MARC-145 cells were infected with the PRRSV, and the cell lysates were subjected to western blotting analysis. As shown in Fig. 4, the pRb abundance in PRRSV-infected MARC-145 cells reduced significantly from 36 h to 60 h post-infection compared with mock-infected cells, indicating that the PRRSV infection can down-regulate the pRb level in MARC-145 cells.

The Nsp9 of genotype 2 PRRSV could promote the degradation of pRb by ubiquitin proteasome pathway

Several studies have shown that many viral proteins that interact with pRb promoted the pRb degradation by ubiquitin proteasome pathway (Bhardwaj et al., 2012; Kalejta et al., 2003; Kehn et al., 2004; Munakata et al., 2007). The fact that the Nsp9 of genotype 2 PRRSV interacts with pRb and the PRRSV infection reduces the pRb level suggests that Nsp9 likely modulates the pRb level by ubiquitin proteasome pathway. To confirm this finding, MARC-145 cells were transduced with the Nsp9-expressing lentiviruses and the pRb level was examined by western blotting. Compared with the GFP-expressing cells, the pRb level was significantly down-regulated in the Nsp9-expressing cells, whereas it recovered when the cells were treated with the proteasome inhibitor MG132 (Fig. 5A), indicating that the Nsp9 of genotype 2 PRRSV promotes the degradation of pRb. To consolidate this finding, HEK 293T cells were co-transfected with a dose-dependent increasing Nsp9 and dose-constant pRb-tru, and the pRb-tru level was examined by western blotting. The results showed that the pRb-tru level reduced gradually as the Nsp9 level increased, and it recovered in the cells treated with MG132 (Fig. 5B), indicating that the Nsp9 of genotype 2 PRRSV can down-regulate the pRb abundance by ubiquitin proteasome pathway.

To determine whether Nsp9 promotes the pRb ubiquitination leading to the pRb degradation, HEK 293T cells were co-transfected with pCMV-Myc-pRb-tru and pCMV-HA-Nsp9, and meanwhile, HEK 293T cells were co-transfected with pCMV-Myc-pRb-tru and pCMV-HA as control. The pRb-tru proteins were immunoprecipitated with an anti-Myc antibody and were then detected with an anti-ubiquitin mAb. Compared with the control group, a clear high-molecular-weight smear of the pRb-tru proteins was observed in the presence of the expressed Nsp9, showing that Nsp9 can mediate the ubiquitination of pRb-tru (Fig. 5C).

Discussion

A number of viruses have been shown to directly or indirectly interact with host cellular proteins to modulate the normal cellular life activities and to facilitate their replications. In this study, we described that the Nsp9 of genotype 2 PRRSV interacted with endogenous and exogenous pRb, one of the key cell-cycle regulating proteins. A conserved motifll-cycle regulating proteins. lar proteins to modulate in the Nsp9-overexpressing cells byRNA-dependent RNA polymerases (Bhardwaj et al., 2012; Corbeil and Branton, 1994; Munakata et al., 2005, 2007; Ran et al., 2013). We found the presence of a conserved motif—LACAE in the Nsp9 of genotype 2 PRRSV by aligning the amino acid sequences of the Nsp9 among 17 representative strains of genotype 2 PRRSV. Our results confirmed that the mutation of the conserved residue (*E*) at the position 419 in this motif fully impacted the interaction between Nsp9 and pRb, whereas the substitution of the conserved residues (L and C) at the position 415 and 417 did not affect this interaction, suggesting that the third conserved residue (E) of the LACAE motif plays an essential role in sustaining the interaction between the Nsp9 of genotype 2 PRRSV and pRb. We found no identical or similar LxCxE motif in the Nsp9 of genotype 1 PRRSV. The pRb has shown interaction with histone deacetylase3 (HDAC3) which lacks the LxCxE-like motif (Dahiya et al., 2000). Thus, whether the Nsp9 of genotype 1 PRRSV interacts with pRb or it shares other motif that binds to pRb needs to be further explored.

A study on mouse hepatitis virus (MHV) showed that the viral protein production was delayed at the presence of the pRb overexpression (Bhardwaj et al., 2012). Our results found that the overexpression of exogenous pRb-tru significantly decreased the replication of genotype 2 PRRSV in MARC-145 cells, and silencing the pRb gene obviously increased the viral replication in MARC-145 cells, suggesting that pRb might function as a restriction factor that inhibits the replication of genotype 2 PRRSV. Similar to HCV (Munakata et al., 2007), our data indicated that the pRb had a reduced level in PRRSV-infected MARC-145 cells, inferring that the decrease of the pRb abundance is likely required for the replication of PRRSV. The pRb has been shown to regulate the cell cycle and the pRb-E2F pathway plays a vital role in cell cycle progression. Previous studies in some RNA viruses have shown that the interaction of viral proteins with pRb could alter the cell cycle progression to create favorable cellular environment that is beneficial for viral replication (Nelson and Tang, 2006; Pietschmann et al., 2001; Scholle et al., 2004). Thus, we propose that the interaction between the Nsp9 of genotype 2 PRRSV and pRb might modulate the pRb-E2F pathway and altered the cell cycle progression which affects the viral replication. Further investigation for this issue will be required.

Viruses can encode some proteins to degrade the restrictive factors of host and to counteract their inhibition activities on viruses by utilizing ubiquitin proteasome pathway. The E6 of human papillomavirus has been shown to degrade the tumor suppressor p53 through ubiquitin proteasome pathway (Freedman and Levine, 1998). The Vif of human immunodeficiency virus-1 (HIV-1) and the Vpx of HIV and simian immunodeficiency virus (SIV) have been indicated to target APOBEC3G and HD domain-containing protein-1 (SAMHD1) for proteasomal degradation, separately (Ahn et al., 2012; Hrecka et al., 2011; Kobayashi, 2005). Our results clearly showed that the Nsp9 of PRRSV could promote the degradation of pRb by the ubiquitin–proteasome pathway. Thus, we suggest that the ubiquitinational degradation of pRb might be an important mechanism for the PRRSV Nsp9 to counteract the pRb function. The E3 ubiquitin ligase has been recognized as an important component of ubiquitin–proteasome pathway (Ciechanover, 1994). Similar to HCV NS5B and CoV-SARS Nsp15 (Bhardwaj et al., 2012; Munakata et al., 2007), we observed that pRb altered its distribution and co-localization with Nsp9 of PRRSV in the cytoplasm following PRRSV infection. Thus, we propose a model that Nsp9 recruited pRb to E3 ligases and modulated E3 ligases dependent degradation of pRb by proteasome pathway in the cytoplasm. It needs to be done to clarify the exact mechanism of the pRb degradation.

The pRb interacts with many cellular regulatory proteins and it participates in cell life activities, including the G1/S transition of cell cycle (Nevins, 1992), NF-IL6 and IL-8 expression during immune response (Chen et al., 1996; Zhang et al., 2000) and cell apoptosis (Morgenbesser et al., 1994; Tsai et al., 1998). A further

exploration of the mechanisms concerning how the PRRSV Nsp9 affects the pRb function will be necessary to obtain a more detailed understanding of the relationship between viral replication and pRb loss *in vitro*.

Taken as a whole, our findings are the first to indicate that the Nsp9 of genotype 2 PRRSV interacted with pRb, and this interaction promoted the pRb degradation by ubiquitin proteasome pathway in the cytoplasm and benefited viral replication *in vitro*, providing a novel insight for understanding the roles of Nsp9 in the replication and pathogenesis of PRRSV.

Materials and methods

Cells, virus and antibodies

Porcine pulmonary alveolar macrophages (PAMs) were prepared as previously described (Zhang et al., 2009) and maintained in RPMI-1640 medium (Invitrogen, Grand Island, NY) supplemented with 10% fetal bovine serum (FBS) (Hyclone Laboratories Inc., South Logan, UT). MARC-145 cells and human embryonic kidney (HEK) 293 T cells were maintained in Dulbecco's modified Eagle medium (DMEM) (Invitrogen) supplemented with 10% FBS at 37 °C. The stock of PRRSV JXwn06 was used in this study (Zhou et al., 2009). Mouse anti-HA monoclonal antibody (mAb) (H3663), mouse anti-Myc mAb (M4439), rabbit anti-Myc mAb (C3956), mouse anti-β-actin mAb (A5441) and MG132 (M7449) were all purchased from Sigma–Aldrich (St. Louis, MO). Mouse anti-pRb mAb (#9309) was purchased from Cell Signaling Technology (Danvers, MA). Rabbit anti-pRb polyclonal antibody (sc-7905) and mouse anti-ubiquitin mAb (P4D1) were purchased from Santa Cruz Biotechnology (Santa Cruz. *CA*). Mouse anti-GFP mAb (66002-1-Ig) and rabbit anti-GFP polyclonal antibody (50430-2-AP) were purchased from Proteintech (Chicago, IL).

Plasmid construction

A 1914-nt cDNA fragment of truncated porcine pRb gene (pRb-tru) was amplified from PAMs by RT-PCR with the designed primers 1F/1R (Table 1) according to the porcine pRb gene sequence available in the GenBank database (accession no. XM_001926853.4). The truncated porcine pRb gene was deduced to encode 638 amino acids (aa301–938) with an LxCxE-binding motif. The amplified product was confirmed by sequencing and then subcloned into a lentiviral expression vector pWPXL (Addgene, Cambridge, MA) to generate the pWPXL-pRb-tru-GFP by Pme//Mlu/sites. The pCMV-Myc-pRb-tru was constructed using pCMV-Myc (Clontech Laboratories Inc., Mountain View, CA) with the primers 2F/2R (Table 1) by Bgl///Not/sites. The Nsp9 gene of PRRSV JXwn06 was amplified by PCR using the plasmid pWSK-JXwn as template (Zhou et al., 2009) and the primers 3F/3R and 4F/4R, respectively (Table 1). The amplified fragments were subcloned into pWPXL and pCMV-HA (Clontech Laboratories Inc.) by Pme//Mlu/ and Bgl///Not/ sites to generate the plasmids pWPXL-Nsp9-GFP and pCMV-HA-Nsp9, respectively. The mutants of the Nsp9 LACAE motif were generated by overlapping PCR. The pWPXL-Nsp9 (L415A/C417A)–GFP and pCMV-Nsp9 (L415A/C417A)–HA plasmids were constructed by using the primers 5F/5R with alanine substitutions of L415 and C417 (Table 1). The pWPXL-Nsp9 (E419K)–GFP and pCMV-Nsp9 (E419K)–HA plasmids were generated by using the primers 6F/6R with lysine substitution of E419 (Table 1). All the constructed plasmids were confirmed by sequencing.

Table 2
Amino acid alignment of the pRb-binding motif in the Nsp9 of genotype 2 PRRSV.

PRRSV strain	GenBank accession no	LxCxE motif
VR-2332	AP046869.1	^{410}NLLYE**LACAE**EHLPS[a]
NVSL 97-7985 IA 1-4-2	AF325691.1	^{410}NLLYE**LACAE**EYLPS
P129	AF494042.1	^{410}NLLYE**LACAE**EHLPS
JA142	AY424271.1	^{410}NLLYE**LACAE**EHLPS
BJ-4	AF331831.1	^{410}NLLYE**LACAE**EHLPS
HB-1(sh)-2002	AY150312.1	^{410}NLLYE**LACAE**EHLPS
CH-1a	AY032626.1	^{410}NLLYE**LACAE**EHLPS
NB/04	FJ536165.1	^{410}NLLYE**LACAE**EHLPS
JXA1-P80	FJ548853.1	^{410}NLLYE**LACAE**GHLPS
MLV RespPRRS/Repro	AF159149.1	^{410}NLLYE**LACAE**EHLPS
Prime pac	DQ779791.1	^{410}NLLYE**LACAE**EHLPS
Ingelvac ATP	DQ988080.1	^{410}NLLYE**LACAE**EHQPS
SP	AF184212.1	^{410}NLLYE**LACAE**EHLPS
TJ	EU860248.1	^{410}NLLYE**LACAE**EHLPS
JXA1	EF112445.1	^{410}NLLYE**LACAE**EHLPS
HuN4	EF635006.1	^{410}NLLYE**LACAE**EHLPS
JXwn06	EF641008.1	^{410}NLLYE**LACAE**EHLPS

[a] The bold characters denote the motif.

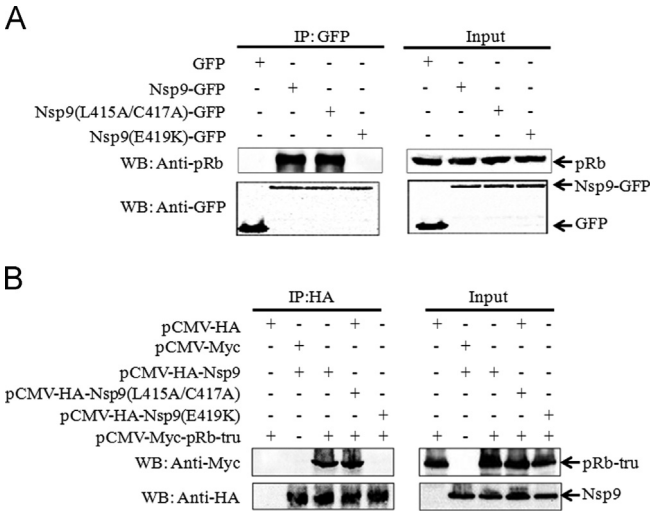

Fig. 1. The interaction between the Nsp9 of genotype 2 PRRSV and pRb. (A) Interaction of Nsp9 with the endogenous pRb. MARC-145 cells were transduced with the lentiviruses expressing GFP, Nsp9, Nsp9 (L415A/C417A) and Nsp9 (E419K) individually. The cell lysates were immunoprecipitated with an anti-GFP mAb and followed by western blotting analysis with anti-pRb and anti-GFP antibodies. The left figure shows the Co-IP analyses of GFP, Nsp9-GFP, Nsp9 (L415A/C417A)–GFP and Nsp9 (E419K)–GFP from cell lysates and the right figure indicates the identification of GFP, Nsp9-GFP, Nsp9 (L415A/C417A)–GFP and Nsp9 (E419K)–GFP expressed in cell lysates. (*B*) Interaction of Nsp9 with the exogenous truncated pRb (pRb-tru). HEK 293T cells were co-transfected with the Myc-pRb-tru-expressing plasmids and the HA-Nsp9-, HA-Nsp9 (L415A/C417A)- or HA-Nsp9 (E419K)-expressing plasmids. The cell lysates were immunoprecipitated with an anti-HA mAb and probed with anti-HA and anti-Myc antibodies. The left figure shows the Co-IP analyses of HA-Nsp9, HA-Nsp9 (L415A/C417A) and HA-Nsp9 (E419K) from cell lysates and the right figure indicates the identification of HA-Nsp9, HA-Nsp9 (L415A/C417A) and HA-Nsp9 (E419K) expressed in cell lysates.

Preparation of Nsp9-, Nsp9 (L415A/C417A)-, Nsp9 (E419K)- and pRb-tru-expressing lentiviruses

A lentiviral packaging system including pWPXL (12257), pMD2.G (12259) and psPAX2 (12260) was available from Addgene. The lentivirus-mediated protein expression was performed according to the standard protocol. Briefly, each fragment of Nsp9, Nsp9 (L415A/C417A), Nsp9 (E419K) and pRb-tru was subcloned into the expression vector pWPXL, respectively. The plasmid pWPXL-Nsp9, pWPXL-Nsp9 (L415A/C417A), pWPXL-Nsp9 (E419K), pWPXL-pRb-tru were mixed with pMD2.G and psPAX2 with appropriate proportion, respectively and were then co-transfected into 80% confluence of HEK 293FT cells using the FuGENE HD Transfection Reagents (Roche Applied Science, Indianapolis, IN). The cells were incubated at 37 °C. After a number of syncytias appeared, the

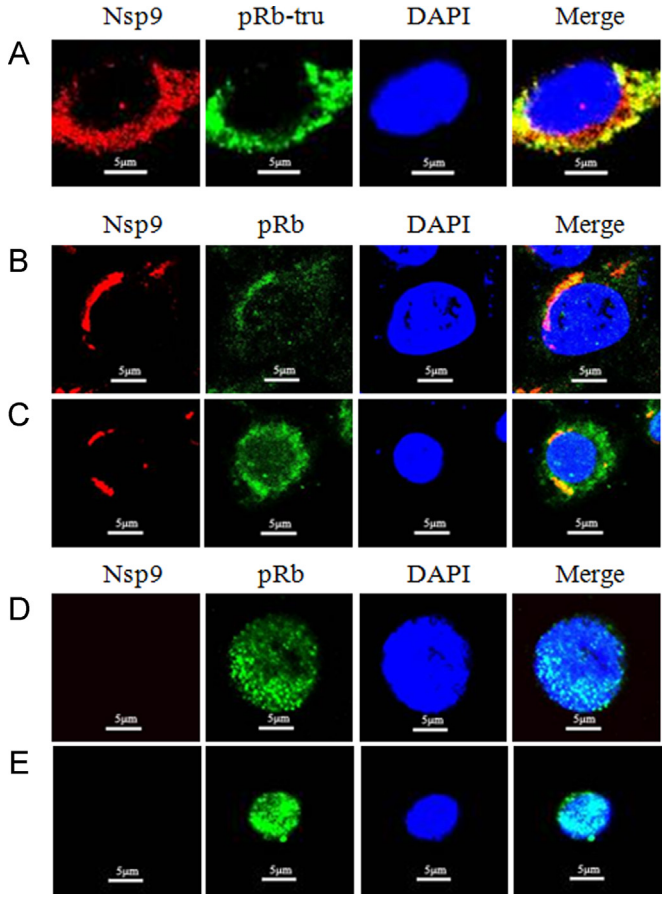

Fig. 2. Co-localization of the Nsp9 of genotype 2 PRRSV with pRb in the cytoplasm. (A) Co-localization of pRb-tru with Nsp9 in MARC-145 cells. MARC-145 cells were co-transfected with pCMV-Myc-pRb-tru and pCMV-HA-Nsp9. The cells were fixed at 36 h post-transfection and processed by immunostaining with a mouse anti-HA mAb or rabbit anti-Myc polyclonal antibody and TRITC-conjugated goat anti-mouse IgG or FITC-conjugated goat anti-rabbit IgG, and were then examined by immunoconfocal microscopy. Nuclei were stained with DAPI. Co-localization of Nsp9 with the endogenous pRb in PRRSV-infected MARC-145 cells (*B*), PRRSV-infected PAMs (C), mock-infected MARC-145 cells (D) and mock-infected PAMs (E). The mock- or PRRSV-infected cells were fixed at 36 h post-infection and processed by immunostaining with a mouse anti-Nsp9 mAb or rabbit anti-pRb polyclonal antibody and TRITC-conjugated goat anti-mouse IgG and FITC-conjugated goat anti-rabbit IgG. Nuclei were stained with DAPI.

supernatants containing lentiviruses were harvested and filtered with a 0.45 filter (Pall Corporation, Port Washington, NY) and were then concentrated by Amicon ultra-100 centrifuge tubes (Mick Millipore, Billerica, MA). The titers of lentiviruses were measured using a QuickTiter™ Lentivirus Titer Kit (Lentivirus-Associated HIV p24) (Cell Biolabs, San Diego, *CA*) and the lentiviruses were stored for use at −80 °C. MARC-145 cells were transduced with the lentiviruses in the presence of 8 μg/mL polybrene (Sigma). Twenty-four hours after the transduction, the inoculums were removed and the cells were maintained in DMEM containing 10% FBS.

Co-immunoprecipitation assay

For the co-immunoprecipitation (Co-IP) assay of the Nsp9 and endogenous pRb, MARC-145 cells were transduced with the lentiviruses that were expressing GFP, Nsp9-GFP, Nsp9 (L415A/C417A)–GFP or Nsp9 (E419K)–GFP in the presence of 8 μg/ mL polybrene, respectively. The cells were harvested and lysed in pre-cooled Co-IP lysis buffer (Beyotime, Shanghai, China) at 36 h post-transduction. The cell lysates were precipitated with a anti-GFP mAb in conjunction with Protein A Sepharose (GE Healthcare, Fairfield, CT) overnight at 4 °C with gentle rotation. The beads were washed three times with the lysis buffer, and were then boiled with 5 × SDS loading buffer (Beyotime) for 5 min. The eluted proteins from the beads were subjected to western blotting analysis using an anti-pRb or anti-GFP mAb. To distinguish light chain and GFP, an anti-GFP polyclonal antibody was used.

For the Co-IP assay of the Nsp9 and exogenous pRb-tru, HEK 293T cells were co-transfected with pCMV-HA-Nsp9 and pCMV-Myc-pRb-tru, pCMV-HA-Nsp9 (L415A/C417A) and pCMV-Myc-pRb-tru, pCMV-HA-Nsp9 (E419K) and pCMV-Myc-pRb-tru, pCMV-HA-Nsp9 and empty vector, or empty vector and pCMV-Myc-pRb-tru, respectively, using a Lipofectamine™ LTX and PLUS™ Reagents (Invitrogen). Thirty-six hours after the transfection, the cells were harvested and lysed in pre-cooled Co-IP lysis buffer. The lysates of cells were subjected to Co-IP assays according to HA-Tag IP/Co-IP Application Set instructions (Thermo Fisher, Waltham, MA). The eluted proteins from the beads were subjected to western blotting analysis using an anti-HA or anti-Myc mAb.

Confocal immunofluorescence assay

For the co-localization analysis of the Nsp9 and exogenous pRb-tru, MARC-145 cells seeded on coverslips in 24-well plates (Corning Inc., Corning, NY) were co-transfected with pCMV-HA-Nsp9 and pCMV-Myc-pRb-tru using the Lipofectamine™ LTX and PLUS™ Reagents when they were grown to approximately 70% confluence. Thirty-six hours after the transfection, the cells were fixed with 100% pre-cooled ethyl alcohol for 15 min at room temperature, and were then washed with PBS for 3 min, and incubated for 1 h at 37 °C with an anti-HA mAb and anti-Myc polyclonal antibody. After washing three times with PBS, the cells were incubated with TRITC-conjugated goat anti-mouse IgG or FITC-conjugated goat anti-rabbit IgG for 1 h at 37 °C. After three washes with PBS, the cells were stained for nuclei with DAPI (Beyotime) for 5 min at room temperature and visualized under a Nikon TE-2000E confocal fluorescence microscope (Nikon Instruments, Inc., Melville, NY).

For the co-localization analysis of the Nsp9 and endogenous pRb, MARC-145 cells and PAMs were infected with the PRRSV JXwn06 at a multiplicity of infection (MOI) of 0.01. Thirty-six hours after the infection, the cells were fixed with 100% pre-cooled ethyl alcohol, and then washed with PBS for 3 min. The cells were probed with an anti-Nsp9 mAb prepared in our laboratory or anti-pRb polyclonal antibody, followed by TRITC-conjugated goat anti-mouse IgG or FITC-conjugated goat anti-rabbit IgG for 1 h at 37 °C. After three washes with PBS, the nuclei were stained with DAPI for 5 min at room temperature and visualized under Nikon TE-2000E confocal fluorescence microscope.

Infection of MARC-145 cells that were expressing pRb-tru with PRRSV

MARC-145 cells that were seeded into 24-well culture plates were transduced with the lentiviruses expressing pRb-tru. Twenty-four hours after the transduction, the inoculums were removed and the cells were washed three times with PBS, and were then infected with the PRRSV JXwn06 at MOI of 0.01 in DMEM with 5% FBS. After 1 h incubation, the inoculums were removed, and the cells were washed three times with PBS and maintained in DMEM containing 5% FBS. The cells were harvested at 24 h, 36 h and 48 h post-infection, and were then frozen and thawed for three times. After the centrifugation, the culture supernatants were collected and the virus titers ($TCID_{50}$) were determined using a microtitation infection assay. Similarly, the MARC-145 cells with silencing pRb gene were infected with the virus as above described.

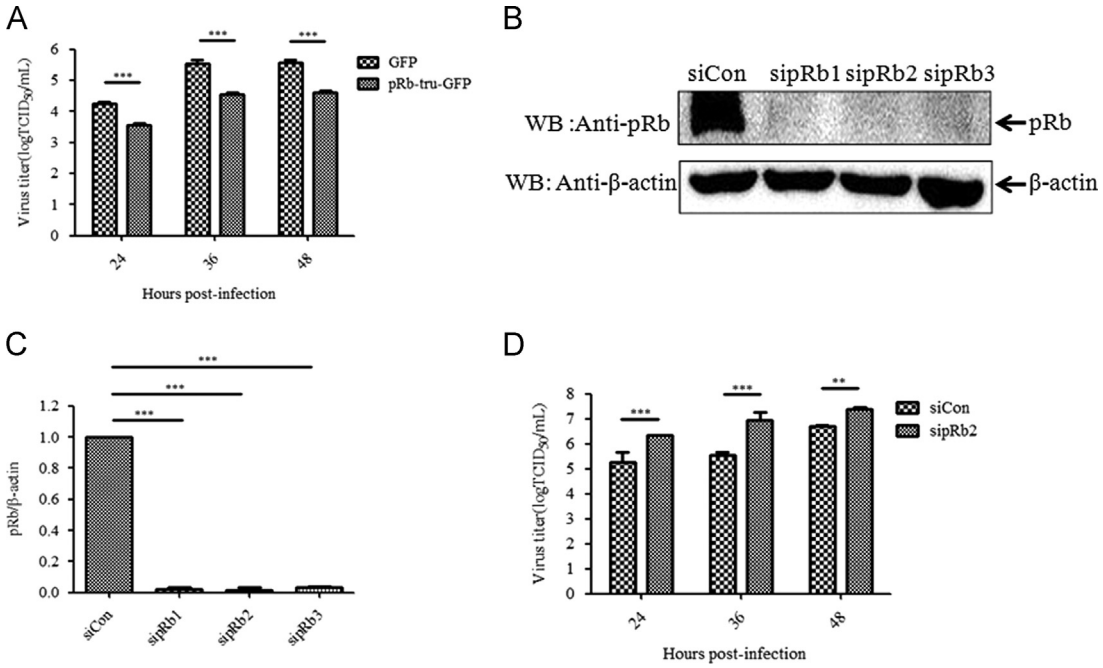

Fig. 3. Inhibition of genotype 2 PRRSV replication by pRb. (A) PRRSV titers in pRb-tru-overexpressed MARC-145 cells. MARC-145 cells were transduced with the lentiviruses expressing GFP and pRb-tru, respectively. The cells were infected with PRRSV JXwn06 at MOI of 0.01 at 24 h post-transduction, and the virus titers were then assayed by a microtitration infectivity assay at the indicated time points post-infection. Data are shown as means ± SD of three independent experiments ($^{**}P < 0.01$; $^{***}P < 0.001$). (B) Effect of silencing the pRb gene on the abundance of endogenous pRb. MARC-145 cells were transfected with siRNA (sipRb1, sipRb2, sipRb3) and control siRNA (siCon). The cells were harvested at 48 h post-transfection and the cell lysates were probed with an anti-pRb antibody. (C) The optical density ratios of pRb/β-actin in pRb gene-silenced MARC-145 cells are shown with graphs. Data are shown as means ± SD of three independent experiments ($^{***}P < 0.001$). (*D*) PRRSV titers in pRb gene-silenced MARC-145 cells. MARC-145 cells transfected with the siRNA (sipRb2) or control siRNA (siCon) for 48 h were infected with PRRSV JXwn06 at MOI of 0.01, and the virus titers were assayed at the indicated time points post-infection. Data are shown as means ± SD of three independent experiments ($^{**}P < 0.01$; $^{***}P < 0.001$).

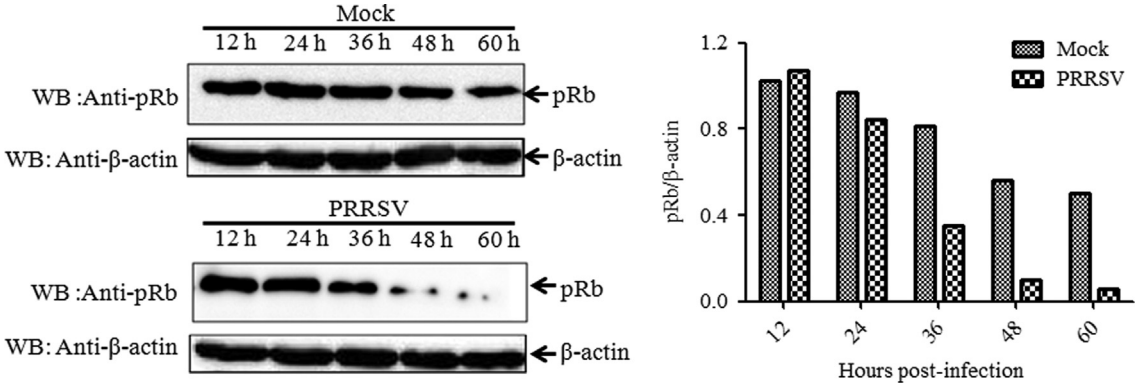

Fig. 4. Down-regulation of the pRb level in genotype 2 PRRSV-infected MARC-145 cells. MARC-145 cells infected with PRRSV JXwn06 at MOI of 0.01 were harvested at the indicated time points post-infection, and the cell lysates were then probed with an anti-pRb antibody. The optical density ratios of pRb/β-actin are shown with graphs.

Silencing pRb gene with siRNA

The siRNA for silencing pRb gene were purchased from Shanghai GenePharma (Shanghai, China). MARC-145 cells were treated with 30 pmol of siRNA using the Lipofectamine RNAiMax (Invitrogen) according to the manufacturer's instructions. Forty-eight hours after the treatment, the cell lysates were subjected to western blotting analysis using an anti-pRb antibody. The siRNA target sequences were as follows: sipRb1 (sense), 5′- GGACAUGUGAACUUAUAUATT -3′; sipRb2 (sense), 5′- GCUCUCAGAUUCACCUUUATT -3′; sipRb3 (sense), 5′–CCAGAAGC-CAUUGAAAUCUTT-3′; the control siCon (sense), 5′–UUGCGGGUCUAAU-CACCGATT-3′.

Infection of MARC-145 cells with PRRSV

MARC-145 cells seeded into 6-well culture plates (Corning Inc.) were infected with the PRRSV at MOI of 0.01 in DMEM with 5% FBS. The cells were harvested at 12 h, 24 h, 36 h, 48 h, and 60 h post-infection. The cell lysates were subjected to western blotting analysis using an anti-pRb antibody. Meanwhile, the lysates of mock-infected cells were served as the control.

pRb degradation assay

For the endogenous pRb degradation assay, the MARC-145 cells seeded into 6-well culture plates were transduced with the lentiviruses that were expressing Nsp9 or GFP in the presence of 8 μg/mL polybrene. After 24 h, the inoculums were removed and replaced with DMEM containing 10% FBS. The cells were treated with DMSO or 10 μM MG132 for 12 h. The cell lysates were then harvested and subjected to western blotting analysis using an anti-pRb and anti-GFP antibody.

For the exogenous pRb degradation assay, HEK 293T cells seeded into 6-well culture plates were co-transfected with the

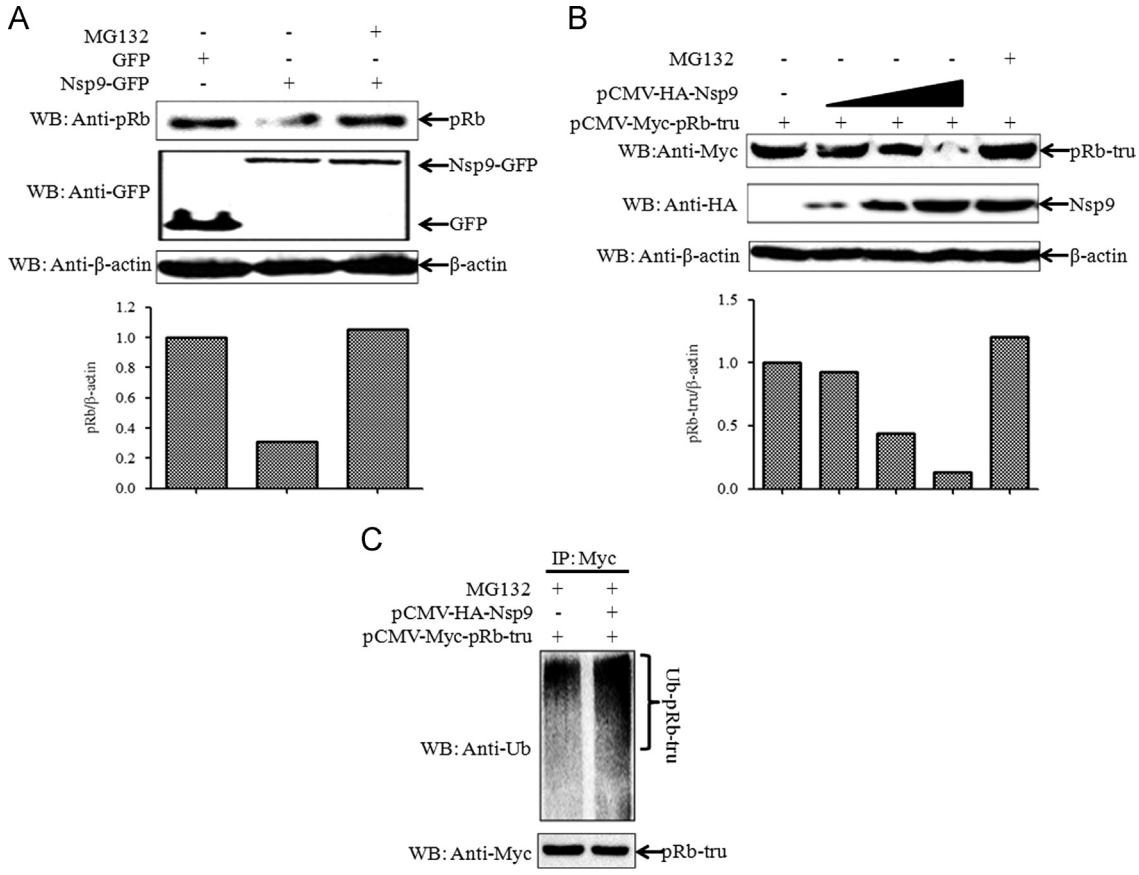

Fig. 5. Down-regulation of the pRb level in the Nsp9-overexpressing cells by ubiquitin proteasome pathway. (A) Down-regulation of the pRb level by Nsp9 in MARC-145 cells. MARC-145 cells were tranduced with the GFP- or Nsp9-expressing lentiviruses. The cells were treated with 10 μM DMSO or MG132 and the cell lysates were then harvested for western blotting analysis. The optical density ratios of pRb/β-actin are shown with graphs. (B) Down-regulation of pRb-tru by Nsp9 in HEK 293T cells. HEK 293T cells were co-transfected with a constant dose of pCMV-Myc-pRb-tru and different dose of pCMV-HA-Nsp9. The cells were then treated with 10 μM DMSO or MG132, and the cell lysates were harvested for western blotting analysis with an anti-Myc or anti-HA antibody. The optical density ratios of pRb-tru/β-actin are shown with graphs. (C) Modulation of the ubiquitination of pRb-tru by Nsp9 in HEK 293T cells. HEK 293T cells were co-transfected with the pCMV-Myc-pRb-tru and pCMV-HA-Nsp9. The cells were then treated with DMSO or 10 μM MG132, and the cell lysates were immunoprecipitated with an anti-Myc antibody and probed with anti-ubiquitin and anti-Myc antibodies.

constant pCMV-Myc-pRb-tru (0.5 μg) and dose-dependent pCMV-HA-Nsp9 (0 μg, 0.5 μg, 1 μg, 1.5 μg, 1.5 μg). The cells were treated with DMSO or 10 μM MG132 for 12 h. The cell lysates were then harvested and subjected to western blotting analysis using an anti-HA or anti-Myc antibody.

The pRb ubiquitination assay

HEK 293T cells seeded into 20 cm^2 cell culture dish (Corning Inc.) were co-transfected with 3 μg of pCMV-Myc-pRb-tru and 9 μg of pCMV-HA-Nsp9 or empty vector. The cells were treated with 10 μM MG132 for 12 h. The cell lysates were then precipitated with an anti-Myc mAb in conjunction with Protein A Sepharose overnight at 4 °C with gentle rotation. The beads were washed three times with the lysing buffer, and were then boiled with 5 × SDS loading buffer for 5 min. The eluted proteins were used for western blotting analysis using an anti-ubiquitin mAb.

Statistical analysis

The data were expressed as means ± standard deviations (SD). Statistical significance among different groups was determined by Two-way ANOVA test of variance using the GraphPad Prism software (version 5.0). A $P < 0.05$ was considered to be statistically significant.

Acknowledgments

This study was supported by Key project of National Natural Science Funds from National Natural Science Foundation of China (31330077) and National Key Basic Research Plan Grant (2014CB542700) from the Chinese Ministry of Science and Technology, and the earmarked fund for Modern Agro-industry Technology Research System of China (CARS-36) from the Chinese Ministry of Agriculture.

References

Ahn, J., Hao, C., Yan, J., DeLucia, M., Mehrens, J., Wang, C., Gronenborn, A.M., Skowronski, J., 2012. HIV/simian immunodeficiency virus (SIV) accessory virulence factor vpx loads the host cell restriction factor SAMHD1 onto the E3 ubiquitin ligase complex CRL4DCAF1. J. Biol. Chem. 287 (15), 12550–12558.

Beura, L.K., Dinh, P.X., Osorio, F.A., Pattnaik, A.K., 2011. Cellular poly(C) binding proteins 1 and 2 interact with porcine reproductive and respiratory syndrome virus nonstructural protein 1 and support viral replication. J. Virol. 85 (24), 12939–12949.

Beura, L.K., Sarkar, S.N., Kwon, B., Subramaniam, S., Jones, C., Pattnaik, A.K., Osorio, F.A., 2010. Porcine reproductive and respiratory syndrome virus nonstructural protein 1beta modulates host innate immune response by antagonizing IRF3 activation. J. Virol. 84 (3), 1574–1584.

Bhardwaj, K., Liu, P., Leibowitz, J.L., Kao, C.C., 2012. The coronavirus endoribonuclease Nsp15 interacts with retinoblastoma tumor suppressor protein. J. Virol. 86 (8), 4294–4304.

Boyer, S.N., Wazer, D.E., Band, V., 1996. E7 protein of human papilloma virus-16 induces degradation of retinoblastoma protein through the ubiquitin-proteasome pathway. Cancer Res. 56 (20), 4620–4624.

Cavanagh, D., 1997. Nidovirales: a new order comprising coronaviridae and arteriviridae. Arch. Virol. 142 (3), 629–633.
Chen, P.L., Riley, D.J., Chen-Kiang, S., Lee, W.H., 1996. Retinoblastoma protein directly interacts with and activates the transcription factor NF-IL6. Proc. Natl. Acad. Sci. U. S. A. 93 (1), 465–469.
Ciechanover, A., 1994. The ubiquitin-proteasome proteolytic pathway. Cell 79 (1), 13–21.
Conzelmann, K.K., Visser, N., Van Woensel, P., Thiel, H.J., 1993. Molecular characterization of porcine reproductive and respiratory syndrome virus, a member of the arterivirus group. Virology 193 (1), 329–339.
Corbeil, H.B., Branton, P.E., 1994. Functional importance of complex formation between the retinoblastoma tumor suppressor family and adenovirus E1A proteins as determined by mutational analysis of E1A conserved region 2. J. Virol. 68 (10), 6697–6709.
Dahiya, A., Gavin, M.R., Luo, R.X., Dean, D.C., 2000. Role of the LXCXE binding site in Rb function. Mol. Cell. Biol. 20 (18), 6799–6805.
den Boon, J.A., Faaberg, K.S., Meulenberg, J.J., Wassenaar, A.L., Plagemann, P.G., Gorbalenya, A.E., Snijder, E.J., 1995. Processing and evolution of the N-terminal region of the arterivirus replicase ORF1a protein: identification of two papain-like cysteine proteases. J. Virol. 69 (7), 4500–4505.
Fang, Y., Snijder, E.J., 2010. The PRRSV replicase: exploring the multifunctionality of an intriguing set of nonstructural proteins. Virus Res. 154 (1-2), 61–76.
Fang, Y., Treffers, E.E., Li, Y., Tas, A., Sun, Z., van der Meer, Y., de Ru, A.H., van Veelen, P.A., Atkins, J.F., Snijder, E.J., Firth, A.E., 2012. Efficient-2 frameshifting by mammalian ribosomes to synthesize an additional arterivirus protein. Proc. Natl. Acad. Sci. U. S. A. 109 (43), E2920–E2928.
Firth, A.E., Zevenhoven-Dobbe, J.C., Wills, N.M., Go, Y.Y., Balasuriya, U.B., Atkins, J.F., Snijder, E.J., Posthuma, C.C., 2011. Discovery of a small arterivirus gene that overlaps the GP5 coding sequence and is important for virus production. J. Gen. Virol. 92 (Pt 5), 1097–1106.
Forng, R.Y., Atreya, C.D., 1999. Mutations in the retinoblastoma protein-binding LXCXE motif of rubella virus putative replicase affect virus replication. J. Gen. Virol. 80 (Pt 2), 327–332.
Freedman, D.A., Levine, A.J., 1998. Nuclear export is required for degradation of endogenous p53 by MDM2 and human papillomavirus E6. Mol. Cell. Biol. 18 (12), 7288–7293.
Garner, M.G., Whan, I.F., Gard, G.P., Phillips, D., 2001. The expected economic impact of selected exotic diseases on the pig industry of Australia. Rev. Sci. Tech. 20 (3), 671–685.
Han, M., Du, Y., Song, C., Yoo, D., 2013. Degradation of CREB-binding protein and modulation of type I interferon induction by the zinc finger motif of the porcine reproductive and respiratory syndrome virus nsp1alpha subunit. Virus Res. 172 (1-2), 54–65.
Hrecka, K., Hao, C., Gierszewska, M., Swanson, S.K., Kesik-Brodacka, M., Srivastava, S., Florens, L., Washburn, M.P., Skowronski, J., 2011. Vpx relieves inhibition of HIV-1 infection of macrophages mediated by the SAMHD1 protein. Nature 474 (7353), 658–661.
Johnson, C.R., Griggs, T.F., Gnanandarajah, J., Murtaugh, M.P., 2011. Novel structural protein in porcine reproductive and respiratory syndrome virus encoded by an alternative ORF5 present in all arteriviruses. J. Gen. Virol. 92 (Pt 5), 1107–1116.
Kalejta, R.F., Bechtel, J.T., Shenk, T., 2003. Human cytomegalovirus pp71 stimulates cell cycle progression by inducing the proteasome-dependent degradation of the retinoblastoma family of tumor suppressors. Mol. Cell. Biol. 23 (6), 1885–1895.
Kehn, K., Fuente, C., d.l. Strouss, K., Berro, R., Jiang, H., Brady, J., Mahieux, R., Pumfery, A., Bottazzi, M.E., Kashanchi, F., 2004. The HTLV-I tax oncoprotein targets the retinoblastoma protein for proteasomal degradation. Oncogene 24 (4), 525–540.
Khidr, L., Chen, P.L., 2006. RB, the conductor that orchestrates life, death and differentiation. Oncogene 25 (38), 5210–5219.
Kim, O., Sun, Y., Lai, F.W., Song, C., Yoo, D., 2010. Modulation of type I interferon induction by porcine reproductive and respiratory syndrome virus and degradation of CREB-binding protein by non-structural protein 1 in MARC-145 and HeLa cells. Virology 402 (2), 315–326.
Kobayashi, M., 2005. Ubiquitination of APOBEC3G by an HIV-1 Vif-Cullin5-Elongin B-Elongin C complex is essential for Vif function. J. Biol. Chem. 280 (19), 18573–18578.
Li, J., Guo, D., Huang, L., Yin, M., Liu, Q., Wang, Y., Yang, C., Liu, Y., Zhang, L., Tian, Z., Cai, X., Yu, L., Weng, C., 2014. The interaction between host annexin A2 and viral Nsp9 is beneficial for replication of porcine reproductive and respiratory syndrome virus. Virus Res. 189C, 106–113.
Li, Y., Zhou, L., Zhang, J., Ge, X., Zhou, R., Zheng, H., Geng, G., Guo, X., Yang, H., 2014. Nsp9 and Nsp10 contribute to the fatal virulence of highly pathogenic porcine reproductive and respiratory syndrome virus emerging in China. PLoS Pathog. 10 (7), e1004216.
Meng, X.J., Paul, P.S., Halbur, P.G., Lum, M.A., 1995. Phylogenetic analyses of the putative M (ORF 6) and N (ORF 7) genes of porcine reproductive and respiratory syndrome virus (PRRSV): implication for the existence of two genotypes of PRRSV in the U.S.A. and Europe. Arch. Virol. 140 (4), 745–755.
Morgenbesser, S.D., Williams, B.O., Jacks, T., DePinho, R.A., 1994. p53-dependent apoptosis produced by Rb-deficiency in the developing mouse lens. Nature 371 (6492), 72–74.
Munakata, T., Liang, Y., Kim, S., McGivern, D.R., Huibregtse, J., Nomoto, A., Lemon, S.M., 2007. Hepatitis C virus induces E6AP-dependent degradation of the retinoblastoma protein. PLoS Pathog. 3 (9), e139.
Munakata, T., Nakamura, M., Liang, Y., Li, K., Lemon, S.M., 2005. Down-regulation of the retinoblastoma tumor suppressor by the hepatitis C virus NS5B RNA-dependent RNA polymerase. Proc. Natl. Acad. Sci. U. S. A. 102 (50), 18159–18164.
Nelson, E.A., Christopher-Hennings, J., Drew, T., Wensvoort, G., Collins, J.E., Benfield, D.A., 1993. Differentiation of U.S. and European isolates of porcine reproductive and respiratory syndrome virus by monoclonal antibodies. J. Clin. Microbiol. 31 (12), 3184–3189.
Nelson, H.B., Tang, H., 2006. Effect of cell growth on hepatitis C virus (HCV) replication and a mechanism of cell confluence-based inhibition of HCV RNA and protein expression. J. Virol. 80 (3), 1181–1190.
Neumann, E.J., Kliebenstein, J.B., Johnson, C.D., Mabry, J.W., Bush, E.J., Seitzinger, A.H., Green, A.L., Zimmerman, J.J., 2005. Assessment of the economic impact of porcine reproductive and respiratory syndrome on swine production in the United States. J. Am. Vet. Med. Assoc. 227 (3), 385–392.
Nevins, J.R., 1992. E2F: a link between the Rb tumor suppressor protein and viral oncoproteins. Science 258 (5081), 424–429.
Pedersen, K.W., van der Meer, Y., Roos, N., Snijder, E.J., 1999. Open reading frame 1a-encoded subunits of the arterivirus replicase induce endoplasmic reticulum-derived double-membrane vesicles which carry the viral replication complex. J. Virol. 73 (3), 2016–2026.
Pejsak, Z., Stadejek, T., Markowska-Daniel, I., 1997. Clinical signs and economic losses caused by porcine reproductive and respiratory syndrome virus in a large breeding farm. Vet. Microbiol. 55 (1-4), 317–322.
Pietschmann, T., Lohmann, V., Rutter, G., Kurpanek, K., Bartenschlager, R., 2001. Characterization of cell lines carrying self-replicating hepatitis C virus RNAs. J. Virol. 75 (3), 1252–1264.
Ran, X., Bian, X., Ji, Y., Yan, X., Yang, F., Li, F., 2013. White spot syndrome virus IE1 and WSV056 modulate the G1/S transition by binding to the host retinoblastoma protein. J. Virol. 87 (23), 12576–12582.
Scholle, F., Li, K., Bodola, F., Ikeda, M., Luxon, B.A., Lemon, S.M., 2004. Virus-host cell interactions during hepatitis C virus RNA replication: impact of polyprotein expression on the cellular transcriptome and cell cycle association with viral RNA synthesis. J. Virol. 78 (3), 1513–1524.
Snijder, E.J., Meulenberg, J.J., 1998. The molecular biology of arteriviruses. J. Gen. Virol. 79 (Pt 5), 961–979.
Sun, Z., Chen, Z., Lawson, S.R., Fang, Y., 2010. The cysteine protease domain of porcine reproductive and respiratory syndrome virus nonstructural protein 2 possesses deubiquitinating and interferon antagonism functions. J. Virol. 84 (15), 7832–7846.
Sun, Z., Li, Y., Ransburgh, R., Snijder, E.J., Fang, Y., 2012. Nonstructural protein 2 of porcine reproductive and respiratory syndrome virus inhibits the antiviral function of interferon-stimulated gene 15. J. Virol. 86 (7), 3839–3850.
Tian, K., Yu, X., Zhao, T., Feng, Y., Cao, Z., Wang, C., Hu, Y., Chen, X., Hu, D., Tian, X., Liu, D., Zhang, S., Deng, X., Ding, Y., Yang, L., Zhang, Y., Xiao, H., Qiao, M., Wang, B., Hou, L., Wang, X., Yang, X., Kang, L., Sun, M., Jin, P., Wang, S., Kitamura, Y., Yan, J., Gao, G.F., 2007. Emergence of fatal PRRSV variants: unparalleled outbreaks of atypical PRRS in China and molecular dissection of the unique hallmark. PLoS One 2 (6), e526.
Tripp, R., Ma, Z., Wang, Y., Zhao, H., Xu, A.-T., Wang, Y., Tang, J., Feng, W.-h., 2013. Porcine reproductive and respiratory syndrome virus nonstructural protein 4 induces apoptosis dependent on its 3C-Like serine protease activity. PLoS One 8 (7), e69387.
Tsai, K.Y., Hu, Y., Macleod, K.F., Crowley, D., Yamasaki, L., Jacks, T., 1998. Mutation of E2f-1 suppresses apoptosis and inappropriate S phase entry and extends survival of Rb-deficient mouse embryos. Mol. Cell 2 (3), 293–304.
van Aken, D., Zevenhoven-Dobbe, J., Gorbalenya, A.E., Snijder, E.J., 2006. Proteolytic maturation of replicase polyprotein pp1a by the nsp4 main proteinase is essential for equine arteritis virus replication and includes internal cleavage of nsp7. J. Gen. Virol. 87 (Pt 12), 3473–3482.
van Dinten, L.C., Wassenaar, A.L., Gorbalenya, A.E., Spaan, W.J., Snijder, E.J., 1996. Processing of the equine arteritis virus replicase ORF1b protein: identification of cleavage products containing the putative viral polymerase and helicase domains. J. Virol. 70 (10), 6625–6633.
Wang, L., He, Q., Gao, Y., Guo, X., Ge, X., Zhou, L., Yang, H., 2012. Interaction of cellular poly(C)-binding protein 2 with nonstructural protein 1β is beneficial to Chinese highly pathogenic porcine reproductive and respiratory syndrome virus replication. Virus Res. 169 (1), 222–230.
Wassenaar, A.L., Spaan, W.J., Gorbalenya, A.E., Snijder, E.J., 1997. Alternative proteolytic processing of the arterivirus replicase ORF1a polyprotein: evidence that NSP2 acts as a cofactor for the NSP4 serine protease. J. Virol. 71 (12), 9313–9322.
Weinberg, R.A., 1995. The retinoblastoma protein and cell cycle control. Cell 81 (3), 323–330.
White, M.K., Khalili, K., 2006. Interaction of retinoblastoma protein family members with large T-antigen of primate polyomaviruses. Oncogene 25 (38), 5286–5293.
Whyte, P., Buchkovich, K.J., Horowitz, J.M., Friend, S.H., Raybuck, M., Weinberg, R.A., Harlow, E., 1988. Association between an oncogene and an anti-oncogene: the adenovirus E1A proteins bind to the retinoblastoma gene product. Nature 334 (6178), 124–129.
Zhang, H., Guo, X., Ge, X., Chen, Y., Sun, Q., Yang, H., 2009. Changes in the cellular proteins of pulmonary alveolar macrophage infected with porcine reproductive and respiratory syndrome virus by proteomics analysis. J. Proteome Res. 8 (6), 3091–3097.
Zhang, H., Wei, S., Sun, J., Coppola, D., Zhong, B., Wu, G.D., Goodwin, B., Sebti, S., Djeu, J.Y., Blanck, G., 2000. Retinoblastoma protein activation of interleukin

8 expression inhibits tumor cell survival in nude mice. Cell Growth Differ. 11 (12), 635–639.
Zhou, L., Yang, H., 2010. Porcine reproductive and respiratory syndrome in China. Virus Res. 154 (1-2), 31–37.
Zhou, L., Yang, X., Tian, Y., Yin, S., Geng, G., Ge, X., Guo, X., Yang, H., 2014. Genetic diversity analysis of genotype 2 porcine reproductive and respiratory syndrome viruses emerging in recent years in China. BioMed. Res. Int. 2014, 1–13.
Zhou, L., Zhang, J., Zeng, J., Yin, S., Li, Y., Zheng, L., Guo, X., Ge, X., Yang, H., 2009. The 30-amino-acid deletion in the Nsp2 of highly pathogenic porcine reproductive and respiratory syndrome virus emerging in China is not related to its virulence. J. Virol. 83 (10), 5156–5167.
Zhou, Y., Zheng, H., Gao, F., Tian, D., Yuan, S., 2011. Mutational analysis of the SDD sequence motif of a PRRSV RNA-dependent RNA polymerase. Sci. China Life Sci. 54 (9), 870–879.